

2025 | 500

Experimental study on macroscopic characteristics of free and impingement spray of low diesel temper

Fuel Injection & Gas Admission and Engine Components

Liyan Zhao, Kunming University of Science and Technology

Jilin Lei, Kunming University of Science and Technology, Kunming
Yi Liu, Kunming University of Science and Technology, Kunming
Xiaopei Liu, Kunming University of Science and Technology, Kunming
Dongfang Wang, Kunming University of Science and Technology, Kunming
Xiwen Deng, Kunming University of Science and Technology, Kunming
Wei Deng, Kunming University of Science and Technology, Kunming
Rui Mo, Kunming Yunnei Power Co., Ltd.
Kang Liu, Kunming Yunnei Power Co., Ltd.

DOI: <https://doi.org/10.5281/zenodo.15209665>

This paper has been presented and published at the 31st CIMAC World Congress 2025 in Zürich, Switzerland. The CIMAC Congress is held every three years, each time in a different member country. The Congress program centres around the presentation of Technical Papers on engine research and development, application engineering on the original equipment side and engine operation and maintenance on the end-user side. The themes of the 2025 event included Digitalization & Connectivity for different applications, System Integration & Hybridization, Electrification & Fuel Cells Development, Emission Reduction Technologies, Conventional and New Fuels, Dual Fuel Engines, Lubricants, Product Development of Gas and Diesel Engines, Components & Tribology, Turbochargers, Controls & Automation, Engine Thermodynamics, Simulation Technologies as well as Basic Research & Advanced Engineering. The copyright of this paper is with CIMAC. For further information please visit <https://www.cimac.com>.

ABSTRACT

Cold start condition of diesel engines at high-altitude regions or the secondary start condition of piston aviation piston engines during high-altitude flight, fuel temperature drops will bring numerous negative effects to the comprehensive performance of engine. -50# diesel is selected as the test liquid to investigate the development of the free jet spray and impingement spray at approximately 2000m altitude in this work. Some new phenomena are observed from the morphology of low fuel temperature free jet spray. Compared with the normal temperature spray, the low temperature spray has obvious gathering clusters at the centre line of the bottom, there is no split at the bottom of the free jet spray and the overall free jet spray colour becomes lighter. After fuel injecting from the nozzle, a translucent area appears at the side edge. The composition of low fuel temperature and low injection pressure worsens the diffusion of spray, the area and penetration distance both become smaller. With the increase of injection pressure, the influence of fuel temperature on the free jet spray area tends to be stable, and the effects on the penetration distance gradually decreases. For the morphology of impingement spray, the fuel film spread along the wall spread further than the spray entrained, low fuel temperature lead to the distance difference between the wall attached film and the entrainment spray became larger. A shoulder socket structure be observed and a transition zone are found in the impingement spray. With the decrease of fuel temperature, the diffusion front appears the spread outline after adhering to the wall, and the maximum spread distance and the maximum entrainment height are significantly reduced. The influence of high injection pressure on the maximum diffusion distance and the maximum entrainment height of impingement spray is greater in the case of low temperature fuel. Based on results of this study, a more accurate macroscopic spray morphology reference could be provided for numerical simulate research.

1 INTRODUCTION

The secondary start condition [1] of aviation piston engines during high-altitude flight (temperature drop to nearly -40°C at an altitude of 8000m[2]), as well as the cold start condition of diesel powered mechanical products in special environments such as plateaus or low-temperature areas, all involve low-temperature fuel injection and spray combustion processes. Although researchers have extensively researched diesel engine spray and combustion [3][4][5], issues such as poor atomization [6], cold starting difficulty [7], mixture combustion misfire [8][9], and emission deterioration [10] in plateau environments and during cold start at low temperature remain critical challenges to be addressed. The environmental adaptability of diesel engine hinges on fuel combustion, with combustion efficiency being contingent upon spray characteristics. Therefore, conducting in-depth research on diesel spray characteristics under plateau and low temperature conditions holds significant importance for enhancing diesel engine combustion efficiency and reducing emissions.

The characteristics of plateau environment compared to plain are low pressure, low temperature, and low oxygen concentration. The ambient temperature decreasing with increasing altitude. In the low temperature environment, changes in the physical properties of fuel will significantly affect the spray characteristics of diesel engines. For example, changes in density affect the initial momentum of fuel injection, thus affecting the penetration distance of spray, changes in viscosity affect the evaporation and breaking process of spray, and changes in surface tension affect the diameter and velocity of spray droplets [11] [12] [13]. In the cold start conditions of high-altitude diesel engines and piston aviation engines, in addition to maintaining the same combustion chamber wall temperature as the ambient temperature, the fuel is also in a low temperature state. The influence of low temperature fuel on spray characteristics cannot be ignored. As we all know, the characteristics of spray have an important impact on the combustion process [14], and people still lack full understanding of the internal structure and distribution of spray.

Significant progress has been made in high-pressure common rail injection fuel technology, especially in terms of influencing conditions and parameter variation patterns. Injection pressure [15], ambient pressure and density [16] [17], wall temperature [18], injector diameter [19] [20], and fuel physical properties [21] all affect the mixing of air and fuel. Regarding free spray, increasing injection pressure can enhance spray

homogeneous; however, excessive heat dissipation may occur if the injection pressure is too high [22]. Additionally, adjusting the oil injection pressure requires simultaneous consideration of the impact on temperature and injection mass. Increasing injection pressure in high temperature environments has a positive effect, but unstable ignition occurs when pressure increases in low temperature environments [23]. When there is a lot of fuel, lower injection pressure helps stabilize ignition, otherwise, less fuel and higher injection pressure will have a negative impact on ignition [24]. The higher the injection pressure is, the longer the spray penetration distance is, and the greater the fuel viscosity value at low temperature increases the degree of wet wall. Therefore, the diesel engine does not set too high injection pressure under starting conditions, and it is appropriate to set the injection pressure below 100MPa [25].

The pressure of the high-pressure common rail system takes longer to build up in low-temperature environments, as summarized by Ma [26]. He discovered that as fuel temperature drops, spray diffusion becomes more challenging, resulting in shorter penetration distances and smaller cone angles compared to normal temperature fuel. When the pulse width is narrow, fuel temperature significantly impacts injection quality. Wang [27] examined low fuel temperature spraying using a two-split injection strategy. He found that injection quality decreases with lower temperatures, resulting in a spray area slightly smaller than that of normal temperature fuel, and a slower penetration rate. Wei [28] conducted another experiment to study spray entrainment characteristics near the nozzle tip of diesel engines. He observed some large waveform structures at the jet edge, which he believes may be caused by the free jet entraining more air, leading to an enlarged cone angle. Su [29] also attempted to observe biodiesel spray at temperatures above room temperature (27°C ~ 87°C), but the results indicated minimal differences in spray penetration distances. Additionally, Lee [30] focused on studying gasoline spray, obtaining its macroscopic morphology. They described the spray at low fuel temperatures, noting a longer liquid/vapor penetration time and the presence of a split plume near the injector tip.

The development of wall-impingement spray is distinctly different from that of free spray. Previous research has indicated that the overall entrainment intensity of impact spray is marginally higher than that of free spray [31]. Under a background pressure of 5 MPa, the delayed ignition time for impact spray is longer than for

free spray, and the average time integral natural luminosity of wall-impingement spray is lower than that of free spray [32]. Notably, the collision between the spray and the wall diminished fuel evaporation and air mixing. Reducing the distance between the wall and the injector hinders natural ignition and combustion [33]. Dai [34] proved that low-temperature fuel increased the impinge rate of spray on the wall, and more gaseous spray concentrated at the position before the impinge on the wall. The drop of fuel temperature reduces the gradient of vapor equivalent concentration. Wang [35] analyzed the concentration and velocity of spray at low fuel temperatures, revealed that as fuel temperature dropped from 0°C to -20°C, the average equivalence ratio near the wall significantly decreased. The diffusion radius of fuel spray upon impinging the wall varies slightly across different temperatures. However, it was noted that the injection pulse width was 0.7ms, spray images were captured 1.2ms after the commencement of fuel injection. This implies that the images were gathered 0.5ms after the injection had ended, rendering these studies non-representative of the spray characteristics during the low-temperature fuel injection phase.

The research on diesel fuel spray remains a crucial component of internal combustion engine studies [21]. To address the cold start issue, a comprehensive understanding of the spray is essential. However, our current knowledge of the characteristics of low-temperature fuel spray under cold start conditions is quite limited. Regarding the development of free and impinging spray, scholars have primarily focused on peripheral parameters such as penetration length, cone angle, diffusion radius, and entrainment height. Naturally, this emphasis is due to the spray at room or high temperatures too enrich. Unfortunately, these studies overlook the spray morphology at low fuel temperatures. Apart from a select few parameters, observing additional details in the enriched spray is challenging. There is still a lack of evidence to determine whether and how the spray structure and distribution influence combustion.

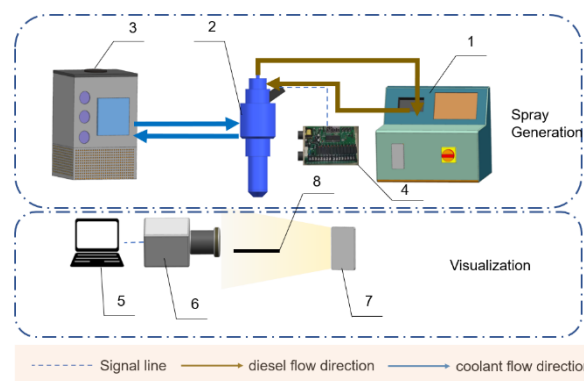
Based on the aforementioned considerations, this study investigated the morphology, typical parameters, and development process of fuel spray at 20 °C, -20 °C, and -40 °C. To prevent solidification and fuel injection failures, -50 diesel was chosen as the primary test fluid. High-speed shadowgraph was employed to capture spray images. By processing these images, analysed the macro spray characteristics of diesel engines and discussed the influence of fuel injection pressure and fuel temperature. This provides

valuable insights for optimizing diesel engine cold start performance.

2 METHODOLOGY EXPERIMENTAL APPARATUS AND PROCEDURES

2.1 Spray Generation and conditions

A schematic diagram of the low-temperature fuel spray test system as illustrated in Fig.1. The spray generation module consists of a fuel preprocessing device, an injector, a pulse controller, and a low-temperature circulating pump. The spray images were obtained through the optical path of the test system, which contained circulating refrigerator, computer, high-speed camera, LED light and wall. The fuel storage and injection pressure control were completed by Borsch fuel preprocessing device, and the injection pressure can be adjusted within the range of 10-180MPa. A nozzle with a diameter of 0.12mm was installed at the bottom of the fuel injector. Under normal temperature, first adjusted the camera, light path and position of nozzle in the picture, adjusted the focus of lens, and calibrated the size with scale. Then, cooled the entire fuel injector to the set temperature with the low-temperature circulating coolant, pressurized the test diesel by the fuel pre-treatment device, triggered signal of the pulse controller to control the fuel injector to inject fuel, and took photos with the camera. The experimental site was in Kunming, with an altitude of about 2000m, an average ambient temperature of 20 °C, the corresponding absolute environmental pressure was 0.081MPa. In this study, the injection pressure of 25MPa, 50MPa, 75MPa and 100MPa was proposed, and the injection pulse width was 2ms. The detailed experimental conditions were shown in Table 1. As the experimental fuel, the -50# diesel was used, and its physicochemical properties were shown in table 2. Before the experiment performed, the temperature inside and outside the injector was calibrated, with a temperature error within $\pm 1^\circ\text{C}$.



1-pretreatment equipment of fuel, 2-injector, 3-circulating refrigerator, 4-controller of pulse, 5-computer, 6-high-speed camera, 7-LED light, 8-wall

Figure 1. Schematic diagram of the low fuel temperature spray test system

Table 1. Characteristics of injector and condition

Item	Value
Injector type	Single-hole
Hole type	Straight hole
Nozzle hole diameter (mm)	0.12
Injection pressure (MPa)	25, 50, 75, 100
Injector and fuel temperature (°C)	20, -20, -40
Pulse width (ms)	2.0
Ambient Temperature (°C)	20
Ambient pressure (MPa)	0.081

Table 2. Main performance of the test diesel

Item	Value
Appearance	Clear & bright
Specific gravity @15°C	0.79 to 0.84 g/ml
Flashing point	-68°C
10% Boiling range	200°C
90% Boiling range	335
Octane number	47

2.2 Visualization

The shadowgraph measurement method has already been proved to measure the spray cone angle and penetration distance more accurately [36], so this technique was used to capture the shadow of the spray. The high-speed camera Fastcam Nova S12 is placed in the same line with the nozzle, and the LED lamp is behind the nozzle. The frame size was 768 x 560 pixels, the interval between the two images was set to 33.3μs, and the exposure time was 1/950000s. The wall was 53mm perpendicular to the nozzle bottom. Then, the blank picture before the first spray image selected as the start time(0μs). Each working condition been tested for 5 times, and the average value was taken for subsequent analysis. The values no units in the figure were all in mm.

Table 3. Details of the optical setup

Parameters	Value
Camera Type	High-speed camera
Resolution (mm)	768x560
Internal Time (μs)	33.33
Exposure time(s)	1/950000
Light source	LED
Position of wall (under the injector) (mm)	53

2.3 Images processing

The image was processed based on programming, the raw images were pre-processed to obtain a grayscale, binarized, edge extracted picture, and then the free jet spray area, spray cone angle, penetration distance, impingement spray morphology, the maximum diffusion distance and the maximum entrainment height were calculated. Fig.2 showed the image processing process, where (a) was the raw free jet spray image obtained from the experiment, (b) was the binarized spray image, and (c) was the edge extracted spray image. The calculation principle of spray penetration distance and cone angle of the free jet were shown in Fig.3(a). The configuration of the impingement spray, the maximum diffusion distance and the maximum entrainment height were shown in 3(b). It should be noted that the free jet spray area is the sum of the pixels occupied by the spray and the penetration distance is calculated as the difference between the start of the spray and the ordinate of the farthest point of the spray, with a cone angle equal to the angle between the spray width at half of the penetration distance and the start point of the spray.

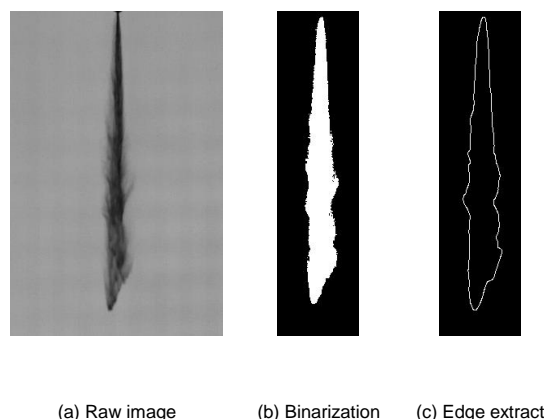


Figure 2. Image processing process

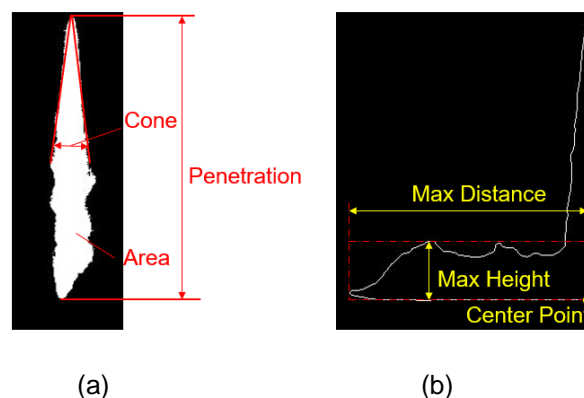


Figure 3. Parameter diagram (a) spray area, penetration distance and cone angle of free spray,

(b) the maximum diffusion distance and the maximum entrainment height of impingement spray

3 RESULTS AND ANALYSIS

3.1 Effect of fuel temperature on morphology of free jet spray

The morphology of the diesel free jet spray under different fuel temperature was presented in this part. As shown in Fig.4, from free jet spray under the condition of the fuel temperature of 20°C、-20°C and -40°C and the injection pressure of 50MPa, similarity can be found first that enrich small darker cluster located at the bottom of spray. Previous studies have observed spray at room temperature or high temperature. Due to the spray too enrich, it was difficult to find this phenomenon. After the fuel injected from the nozzle, under the action of gravity and inertia force, the spray penetration velocity right below the nozzle was the fastest. The stronger the extrusion effect of air resistance, the more the droplets concentrate towards the central line. Therefore, the droplets here were the densest. The initial ignition combustion position of the gas mixture should also be here. This inference can be confirmed from the report of Chen [38].

Then, several distinct differences were found in the spray field. First, as the temperature decreases, the overall spray colour changed from dark to light. To provide a quantitative colour characterization more intuitively, Fig.5 gave the spray total sum darkness of Fig. 4. Compared with 20°C (50MPa), the spray total sum darkness of -40°C(50MPa) was reduced 69.61%、68.79% and 67.88% respectively at 99.99μs, 199.98 and 266.64μs. The spray total sum darkness exhibited an overall similar trend under different fuel temperature conditions. That is, the lower fuel temperature led to smaller darkness of spray.

It is noted that, at 99.99μs, Total darkness of 99.99μs during the development of free spray at -20°C(50MPa) was slightly higher than that at 20°C (50MPa). Because the free jet spray at -20°C appeared mushroom shape at 99.99μs. On the one hand, the penetrate speed was slowed down due to the increase of fuel viscosity and density. On the other hand, the viscous force dominated due to the increase of fuel injection quantity. The resultant force of the inertial force provided by the gravity and fuel injection pressure cannot offset the resultant force of air resistance and viscous force, so the fuel accumulated on the tip and formed a mushroom cloud shape. The shape of

the mushroom cloud increased the contact area between the fuel spray and the air, so the total darkness was slightly more than 20°C. At -40°C, the fuel density became larger, the gravity action dominates, and the combined action with the inertia force is greater than the air resistance, so it continues to penetrated without accumulation. Through analysis, the reason for the difference of spray colour was that (1) more fuel remained in the liquid phase instead of the vapor phase, and the density gradient in the spray is small[39]; (2)the spray is not easy to break and diffuse due to the low temperature, and the diameter of the internal droplets of the spray was larger, the number of droplets was lower[40]; (3) and the shadow method is used for the spray images during the test, and the LED light source is used. The scattering effect of light (the principle of which is shown in Fig. 6) caused the shielding effect of low-density large-diameter droplets on light to be weakened, so the free jet spray colour of low-temperature fuel is lighter.

Second, split pattern in the bottom of free jet spray showed a distinction. At 199.98μs, the bottom of the free jet spray at normal temperature split obviously, and the split degree increased at 266.64μs. While -20°C free jet spray showed a tendency to split at 199.98μs, at 266.64μs it had already split. Correspondingly, the -40°C free jet spray did not split during the displayed time period. This suggests that a decrease in fuel temperature inhibited free jet spray splitting. Because the viscosity and surface tension of low-temperature fuel were larger than that of normal temperature. When encountering the same air resistance, the free jet spray with larger surface tension was not easy to split or break. Another reason is that the free jet spray corresponding to low temperature was narrower and the contact area with air was smaller. The smaller the cross section in contact with the air, the lower the pressure and hence the shear force, so the spray was not easily split.

Third, in the free jet spray at room temperature, almost the translucent shadow area was seen at the upper edge of the spray, and the wave structure was seen at the lower edge, which was almost the same as that observed by Wei [21]. However, after the low-temperature fuel came out of the nozzle, a translucent shadow area can be seen at the side edge. The reason for this field was that the density gradient is generated due to the temperature difference and composition difference between fuel and air [39]. Of course, differences in spray area, penetration and cone angle can also be seen, which will be discussed later.

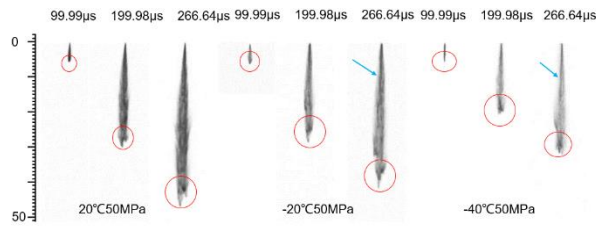


Figure 4. The development of free spray under the injection pressure of 50MPa

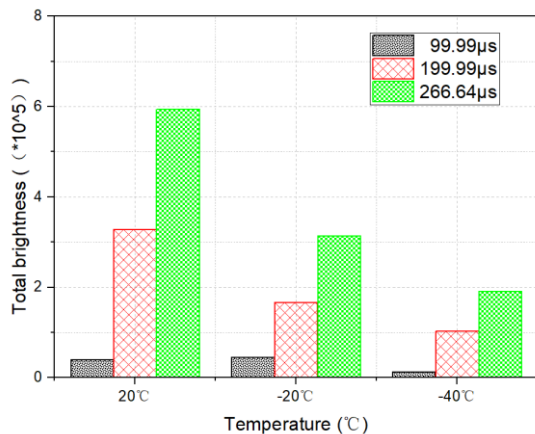


Figure 5. The difference of free spray total darkness at 100MPa

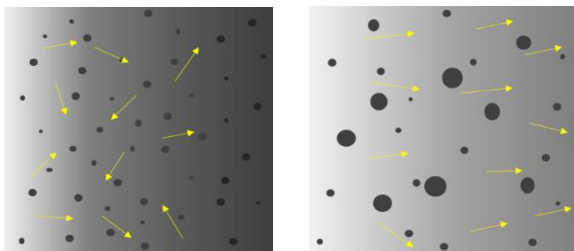


Figure 6. Schematic diagram of shielding effect of different diameters and quantities of droplet spray on light under light scattering

To explain the effect of low temperature and low injection pressure, the free jet spray at injection pressure of 25MPa, 100MPa and different fuel temperature were illustrated in Fig.7. Except the macroscopic features described previously based on Fig.4, as depicted in Fig.7, the spray corresponding to 25MPa at -40°C showed only one linear trace. This also indicated that in the case of an extremely cold start, a lower injection pressure caused fuel injection to fail to form an effective spray. To sum up, the distribution of low-temperature fuel free jet spray was obviously different from that of normal temperature, which has an adverse impact on the combustion of diesel engine in the cold start process [37]. For the optimization of spray, its spatial distribution should be fully considered.

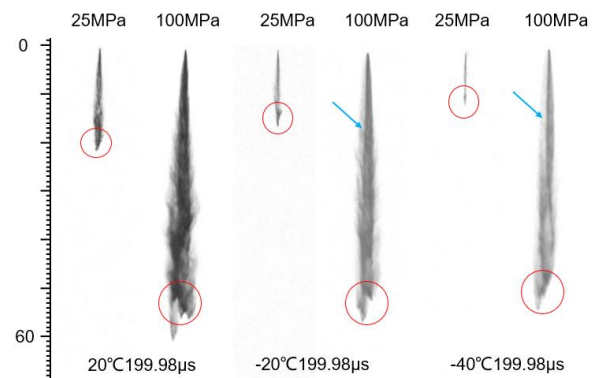


Figure 7. The morphology of free spray at different injection pressure and temperature

3.2 Effect of fuel temperature on characteristic parameters of free jet spray

Quantitative results for the effect of injection pressure and fuel temperature on the free jet spray area and penetration distance were shown in Fig.8 and Fig.9. The fuel injection pulse width was $2000\mu\text{s}$. The time range from the start of fuel injection to the maximum penetration distance of free jet spray not exceeding the screen was $0\sim 666.60\mu\text{s}$. Therefore, the data from the start of fuel injection to $666.60\mu\text{s}$ were selected. It needs to be mentioned that the values were averaged base on 5 repeated cases. It can be seen the free jet spray area and penetration distance gradually increase with time ($0\sim 666.60\mu\text{s}$). In addition, for all cases, two parameters were increase with injection pressure increase or fuel temperature increases. By comparing the deviation of lines in Fig.8 and Fig.9, it can also be concluded that the difference in parameter values between -20°C and -40°C decreases as the injection pressure increase because the distance between the two lines (dashed lines and dotted lines) was closer. This indicates that the increase of fuel injection pressure can compensate for the effect of temperature reduction to a certain extent.

In detail, at $199.98\mu\text{s}$, the free jet spray area of 20°C at 25MPa (Abbreviated as $20^{\circ}\text{C}25\text{MPa}$ in the following) was 132.07mm^2 , while at $-40^{\circ}\text{C}25\text{MPa}$ was 29.53mm^2 , reduced by 77.64%. From 20°C to -40°C , the reduction rate of free jet spray area at injection pressure of 50MPa, 75MPa and 100MPa was 29.65%, 25.25% and 28.46%, respectively. At $299.97\mu\text{s}$, the free jet spray area of $20^{\circ}\text{C}25\text{MPa}$ condition and $-40^{\circ}\text{C}25\text{MPa}$ was 390.01mm^2 and 114.17mm^2 , respectively. With the decrease of temperature, the area decreased by 70.72%; The percentage reduction in free jet spray area at -40°C was 28.11%, 20.34% and 22.61% at 50MPa, 75MPa and 100MPa compared

to 20 °C . In other words, both fuel injection pressure and fuel temperature have impacts on free jet spray diffusion. When the temperature dropped from 20 °C to -40 °C, the spray area was reduced by more than 70% under the low injection pressure of 25MPa, while the free jet spray area was reduced by less than 30% when the injection pressure was increased to 50MPa, 75MPa and 100MPa. This indicated that the effect of fuel temperature on the free jet spray area tends to stabilize with increasing injection pressure. Under low injection pressure, the initial momentum provided by the pressure difference to the fuel is small. When the fuel temperature was reduced to -40 °C, the fuel viscosity and surface tension were increased, restricting the spray to spread around, so the free jet spray area was greatly reduced. With the increase of fuel injection pressure, the circumferential component of initial momentum of fuel leaving the nozzle increases to be far greater than the viscosity and surface tension of fuel at low temperature, so the effect of temperature on the free jet spray area became smaller. When the fuel injection pressure rose to a certain range, the circumferential component no longer increased inconspicuously, so the influence on the free jet spray area tends to be stable.

Then, the influence of fuel temperature and injection pressure on the penetration distance of free jet spray was investigated. At 199.98 μ s, the reduction rate of -40 °C penetration distance on it of 20 °C was 46.20%, 21.84%, 15.32% and 13.91% respectively at four injection pressures. At 299.97 μ s, the reduction in penetration distance was 45.37%, 16.225%, 6.9% and 3.5%, respectively. To sum up, the fuel temperature dropped from 20 °C to -40 °C, and the fuel injection pressure increased from 25MPa to 100MPa. The difference in penetration distance continues to decrease with the superposition of decreasing temperature and increasing injection pressure conditions. It can be concluded that over time the free jet spray penetration distance corresponding to the injection pressure of 100MPa will be close or equal at different fuel temperatures. Different from the change of free jet spray area, the influence of fuel injection pressure on the spray penetration distance was not stable at low temperature, but gradually disappeared. It was because the injection pressure mainly acted on the vertical penetration direction of the free jet spray, while the circumferential diffusion of the spray (represented by the cone angle and area) is mainly influenced by the pressure difference and the cross-sectional area (i.e. diameter) of the nozzle. Therefore, it is different of the influence on free jet spray area and penetration distance. When the fuel injection pressure increased to a certain value, the initial momentum of the fuel was

large enough, then the heat exchange between the spray and the surrounding air was strong enough. As the time elapsed after the fuel leave the nozzle, the spray temperature gradually approached the ambient air, so the difference in penetration distance became smaller and smaller, or even disappeared.

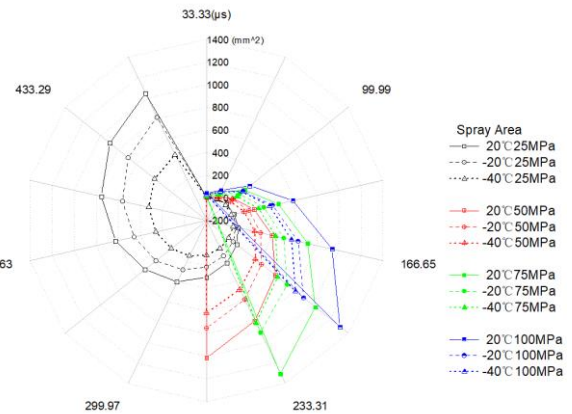


Figure 8. The area of free jet spray at different conditions

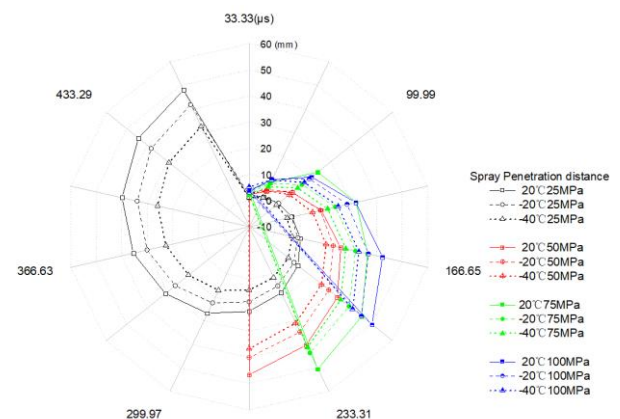


Figure 9. The penetration distance of free jet spray at different conditions

A comparison of free jet spray cone angles under different conditions was shown in Fig. 10. The spray cone angle distribution can be analysed from this box diagram. The horizontal line drawn in the box represented the median value of the data. The height of the box represented the dispersion of the data. The higher the height is, the more dispersed the data is. When the fuel injection pressure was 25MPa, the dispersion degree of the free jet spray cone angle corresponding to 20 °C was the largest, while at 50MPa, 75MPa and 100MPa, the dispersion degree at -40 °C was the largest. At low injection pressures(25MPa), the diameter of the spray droplets was usually larger due to insufficient atomization, resulting in an uncertain taper angle.

As the fuel injection pressure increased, the driving force to the fuel increased. Under the action of gravity, the free jet spray travelled further along the gravity direction, the overall free jet spray shape aspect ratio was larger, and the cone angle was smaller. With the development of free jet spray, the cone angle was gradually stabilized, and the stable value was less than 12° even under different working conditions. At the same time, at the same injection pressure, the stable injection cone angle decreases with the decreases of fuel temperature. Because the decrease in fuel temperature caused an increase in the fuel surface tension and a decrease in the circumferential dispersion of the spray.

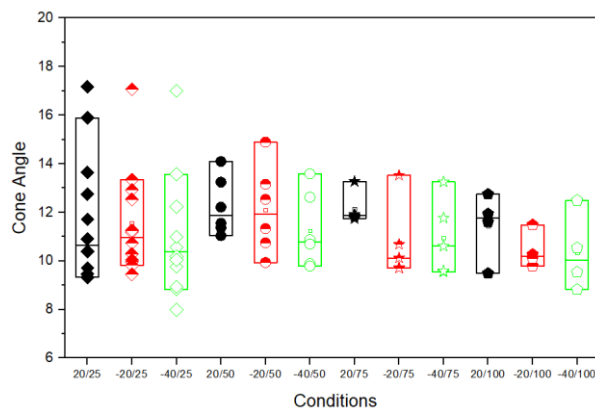


Figure 10. The cone angle of free jet spray at different conditions

3.3 Effect of fuel temperature on the morphology of impingement spray

Impingement spray at normal temperature have been discussed in numerous literatures, while the effect of cold fuel needs further studies. To provide a deep insight to the development of low-temperature fuel impingement spray, the morphology was presented in Fig.11. The first row showed the state of the impingement spray at $999.98\mu\text{s}$ with 25MPa injection pressure, and second row with 100MPa. As the fuel temperature dropped, there are some common features of the impingement spray configuration. First, impingement spray of 20°C rapidly entrained upward while diffusing along the wall. However, at -20°C and -40°C , the impingement spray exchange heat with the wall, and, gradually tending to adhered to the wall and spread, the phenomenon of upward entraining was weakened. It can be seen from the figure that during the process of impingement entrainment, the fuel film spread along the wall spread further than the spray entrained. As the fuel temperature decreased, the distance difference between the wall attached film and the entrainment spray

became larger. There were two reasons for the formation of this structure: one was that the outer edge of the entrained spray was thrown off the wall due to centrifugal force; on the other hand, because the entrainment spray was subjected to gravity in the rising process, part of the fuel fallen onto the wall, secondary wall impingement and diffusion. At -20°C and -40°C , the impingement spray edge was exchange heat with wall and been heated. The decrease in viscosity and increased in diffusion rate provided additional assistance to the attached fuel film [39].

Second, a structure named 'shoulder socket' was found between the main free jet spray and the impinging spray. The reason for the formation of the shoulder socket was that the impingement spray rolled up after impinging the wall. The roll up started from the farthest position and gradually moved closer to the main spray. Therefore, when the entrainment spray did not reach the main spray position, the shoulder socket structure appeared. As the fuel temperature decreased, the size of the shoulder socket structure decreased. As the fuel injection pressure increased, the shoulder socket structure enlarged. As the temperature decreases, it can be seen from the contents in Sections 3.1 and 3.2 that the low-temperature free spray is narrower than the normal temperature spray. Under the same injection pressure and wall impinge distance, the narrow spray has less impact on the wall surface, so the entrained spray moves slower to the main spray, and the entrained height is also lower, forming a smoother shoulder. The increase in fuel injection pressure was equivalent to providing additional impinge force, so the shoulder socket structure was strengthened.

Then, the wave shape was seen in the contour of the entrained spray surface, which was formed by entrained vortices. Dropped the fuel temperature from 20°C to -40°C , the fuel viscosity increased, and the spray that should be entrained and floated warped due to insufficient kinetic energy, so the warping degree increased; However, on the wave-shaped surface of entrainment and floatation, the larger viscous force and surface tension at low temperature restrained the fluctuation of entrainment and floatation spray, so the fluctuation tended to be flat. Compared with the working conditions of different injection pressure under the same temperature, although the trend affected by the temperature is the same, the increased injection pressure can strengthen the diffusion and entrainment of the low-temperature spray after impinged the wall to a certain extent. Optimization of low temperature spray combustion

could be considered starting with the optimization of these structures.

Last, the morphology of impingement spray with time at 100MPa injection pressure were given in Fig.12. At the time stage of 299.97 μ s to 599.97 μ s, on the location where the free jet spray end was connected to the upper end of the impingement spray floated existed a transition region. For a short

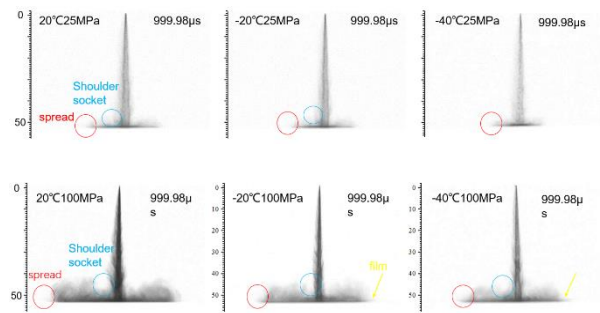


Figure 11. The morphology of impingement spray at different conditions

time after the spray has contacted the wall, a binarized spray plot as shown in Fig.12. It showed that this transition position was approximately rectangular. Over time, as more fuel was injected from the nozzles and added to the impinging process, the transition section gradually became irregular in shape. The analysis suggested that the reason for this transition was that the entrainment of the impingement spray caused the component velocity and force on the vertical wall surface to be upward, creating resistance to the free jet spray. As the temperature decreased, the profile of the transition region became less pronounced. This was because the fuel viscosity at low temperature larger, more fuel adhered to the wall, so the profile characteristics were less obvious than that at normal temperature.

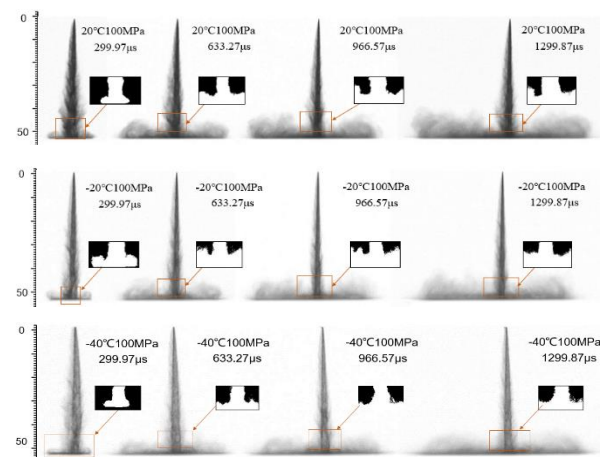


Figure 12. The morphology of impingement spray at different temperatures(100MPa)

3.4 Effect of fuel temperature on characteristic parameters of impingement spray

Fig.13 indicated the maximum diffusion distance and entrainment height of impingement spray at different conditions. Similarly, the values are averaged based on 5 repeated cases. Due to the time of impinged wall was inconsistent, so the timing of nozzle inject fuel was selected as the starting. During the observation period(300 μ s~1900 μ s), the maximum diffusion distance and entrainment height were both decrease with the fuel temperature drop at the four injection pressures.

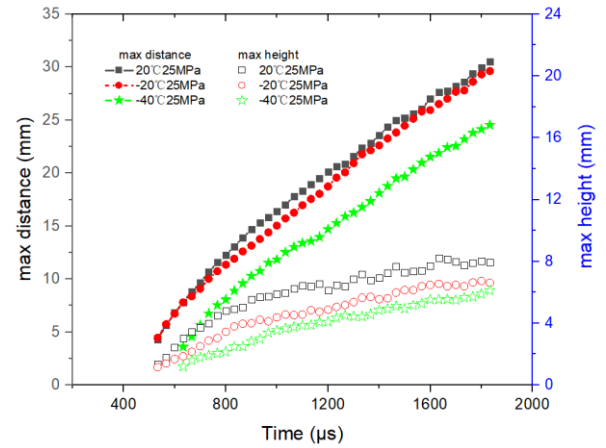
Through the analysis of the maximum diffusion distance of 20 $^{\circ}$ C, -20 $^{\circ}$ C and -40 $^{\circ}$ C at 25MPa, Fig.13(a) exhibited that the maximum diffusion distance of -40 $^{\circ}$ C impingement spray smaller than that of 20 $^{\circ}$ C and -20 $^{\circ}$ C. The two maximum diffusion distance lines overlaps firstly of -20 $^{\circ}$ C and 20 $^{\circ}$ C, and then former is slightly lower than latter after 700 μ s at 25MPa. Fig.13(b) shows that three lines at 500 μ s from coincidence to dispersion at 50MPa. Fig.13(c) illustrated that the time point of changing is 450 μ s at 75MPa. The maximum diffusion distance lines of three fuel temperature start to disperse after 400 μ s at 100MPa, as shown in Fig.13(d). It can be evidently observed by the superimposed fixture at low temperature and low injection pressure worsened the diffusion of impinging spray. Moreover, with the increase of fuel injection pressure, the influence of temperature change on the maximum diffusion distance was earlier. For the reason of this phenomenon was that too less fuel accumulated on the wall at start of fuel injection, this is, only fuel accumulated rather than diffusion. With time gone by, more fuel spray joined in the behaviour of impingement, fuel on the wall splashed and bound, entrained air. With the temperature drop, impingement spray exchange heat with air and lost more energy, larger surface tension consumed more kinetic energy lead to the diffusion velocity and distance smaller.

In addition, this part analysed the composition effect of fuel temperature and injection pressure. As an example, at 1599.84 μ s, at 25MPa, the value of the maximum diffusion distance was 26.99mm(20 $^{\circ}$ C), 25.93mm(-20 $^{\circ}$ C) and 21.52mm(-40 $^{\circ}$ C), respectively. That is, fuel temperature from 20 $^{\circ}$ C dropped to -20 $^{\circ}$ C and -40 $^{\circ}$ C, the maximum diffusion distance reduced 3.92% and 20.26%. At 100MPa, the value of the maximum diffusion distance was 46.93mm(20 $^{\circ}$ C), 45.11mm(-20 $^{\circ}$ C)

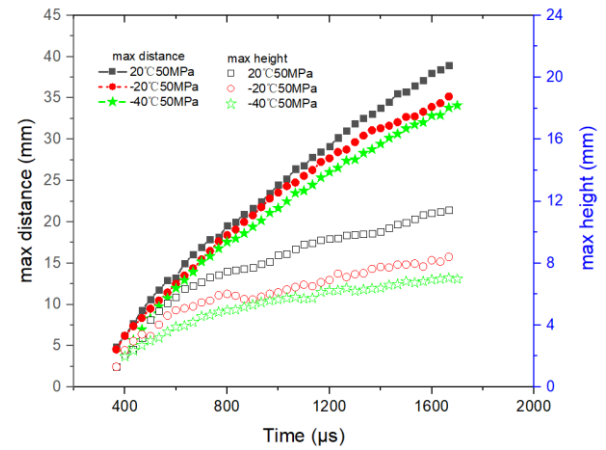
and 40.85mm(-40°C), respectively. That is, fuel temperature from 20°C dropped to -20°C and -40°C, the maximum diffusion distance reduced 3.87% and 12.95%. Wang[35] found the diffusion radius has a little difference of the impingement spray under low fuel temperature. Compared with the composition of low temperature and high pressure, the composition of low temperature and low pressure has a greater impact on the impingement spray. The reason was that under low injection pressure, the kinetic energy of fuel obtained from the nozzle is small, and the viscosity of low-temperature fuel is increased. The superposition of the two impeded the diffusion of impingement spray. When the injection pressure increases, the initial kinetic energy of spray is large, the diffusion speed was accelerated, the heat transfer was strengthened, and the viscosity of spray increases rapidly, so the diffusion distance difference caused by temperature would be shortened.

The composition of fuel temperature and injection pressure has different effects on the maximum entrainment height and the maximum diffusion distance. The condition of low fuel temperature and low injection pressure has a significantly smaller effect on the maximum entrainment height than it at condition of high injection pressure and low temperature. Compared all cases at 1599.84μs: At 25MPa(Fig.12(a)), the maximum entrainment heights were 7.70mm(20 °C), 6.48mm(-20°C) and 5.52mm(-40°C), respectively. Compared with normal temperature, the maximum entrainment height corresponding to the two low temperatures decreased by 15.84% and 23.88%, respectively. At 100MPa(Fig.12(d)), the maximum entrainment height at the three temperatures was 14.99mm (20 °C) , 11.41mm(-20 °C) and 9.61mm(-40 °C), respectively. Compared with normal temperature, the maximum entrainment height of impingement spray caused by low temperature decreased by 28.31% and 35.89%, respectively. Therefore, when the injection pressure increased, the reduction of fuel temperature would lead to a larger proportion of the reduction of the entrainment height of the impingement spray. Under high injection pressure, the evaporation effect of the impingement spray of the normal temperature fuel was strengthened, and the entrainment height was higher, while the entrainment height and diffusion distance of the low-temperature fuel increase under the high injection pressure. Because of the cooling effect of the low-temperature spray on the surrounding air, the gas density near the edge of the spray increased, which resulted in greater resistance to

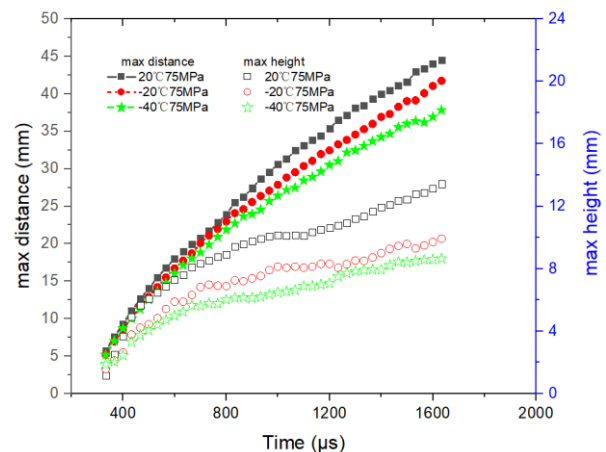
the entrained spray [39], so the difference in the entrainment height was greater.



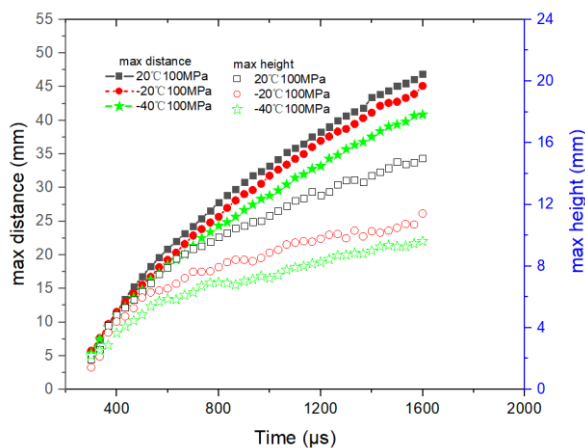
(a)



(b)



(c)



(d)

Figure 13. The maximum diffusion distance and entrainment height of impingement spray at different conditions

4 CONCLUSIONS

The development of low temperature fuel spray is a critical phenomenon for engine cold start, it is undeniable that there is a close relationship between spray morphology and combustion. But the morphology of free jet spray and impingement spray was ignored by researchers. The high-speed shadowgraph was used in this work to get spray pictures at low fuel temperature and different injection pressure conditions. The observation results are summarized as follows.

Some new phenomena were found in the morphology of free jet spray. First, A common phenomenon has been discovered that the enrich darker cluster located at the bottom of spray. Then the colour of spray became lighter with the fuel temperature dropped. Split pattern in the bottom of spray showed a difference. At 20°C, -20°C and -40°C. The bottom of free jet spray pattern was severe split, minor split and no split, respectively. At the edges of the low temperature free jet spray near the tip of the nozzle, a light translucent shadow area was clearly visible and the wave structure became smaller and less. Under the cold start condition of -40 °C , a lower injection pressure(25MPa) may causes fuel injection to fail to form an effective spray.

During the period of injection pulse width, calculated and compared the area and penetration distance of free jet spray. Results showed that the fuel temperature lower, the area and penetration distance smaller. The composition of low fuel temperature and low injection pressure worsen the spray diffusion. High injection pressure has

compensation effect on low temperature fuel free jet spray penetration distance, but not for the area of free jet spray.

The morphology of impingement spray showed some special characteristics at low fuel temperature. First, impingement spray of 20 °C rapidly entrained upward while diffusing along the wall. However, at -20 °C and -40 °C , the impingement spray exchanged heat with the wall, and, gradually tending to adhered to the wall and spread slowly. The fuel film spread along the wall spread further than the spray entrained, low fuel temperature lead to the distance difference between the wall attached film and the entrainment spray became larger. On the connect location where the free jet spray and the impingement spray existed a transition region.

The maximum diffusion distance and the maximum entrainment height were both decreased with the fuel temperature dropped at the four injection pressures during the observation period (300μs~1900μs). By the composing at low temperature and low injection pressure, the diffusion of impingement spray worsened. Moreover, with the increased of fuel injection pressure, the influence of fuel temperature change on the maximum diffusion distance was earlier. The combination of low fuel temperature and low injection pressure has a significantly smaller impact on the maximum entrainment height than the combination of high injection pressure and low temperature. The higher the fuel injection pressure, the greater the influence of low temperature on the maximum entrainment height.

5 ACKNOWLEDGMENTS

This work was supported by the Yunnan Province and Municipal Integration Special Project [grant number 202202AC080004]. Yunnan Fundamental Research Projects [grant number 202301AT070384]. Analysis and Test founding of Kunming University of Science and Technology [grant number 2023P20221106004].

6 REFERENCES AND BIBLIOGRAPHY

- [1] Read, R.W. 2008. Experimental investigations into high-altitude relight of a gas turbine, *University of Cambridge*, Cambridge, UK.
- [2] Mustafa, C. 2021. The international standard atmosphere (ISA).
- [3] Ogawa, H., Ishikawa, T., Kobashi, Y. and Shibata, G. 2024. Influence of spray-to-spray interaction after wall impingement of spray flames

on diesel combustion characteristics, *International Journal of Engine Research*, 25(11): 2032-2044.

[4] Kidoguchi, Y., Ono, M., Noda, Y. and Nada, Y. 2020. Characteristics of Heat Release History of Multi-Hole Diesel Spray Affected by Initial Mixture Formation, Wall Impingement and Spray Interaction, *SAE Powertrains, Fuels & Lubricants Meeting*, Virtual, Online.

[5] Zhan, C. Feng, Z. Ma, W. Zhang, M. Tang, C. and Huang, Z. 2018. Experimental investigation on effect of ethanol and di-ethyl ether addition on the spray characteristics of diesel/biodiesel blends under high injection pressure, *Fuel*, 218(15):1-11.

[6] Zare, A., Bodisco, T.A., Verma, P., Jafari, M., Babaie, M., Yang, L., Rahman, M.M., Banks, A., Ristovski, Z.D., Brown, R.J. and Stevanovic, S. 2020. Emissions and performance with diesel and waste lubricating oil: A fundamental study into cold start operation with a special focus on particle number size distribution, *Energy Conversion & Management*, 209: 112604.

[7] Yang, L.J., Lei, J.L., Wang, Z.J., Wang, D.F., Chen, J.L., Li, D.S., Liu, K. and Sun, L. 2025. Impacts of different ambient temperatures on cold-start characteristics of speed-up duration of an ISAD hybrid diesel engine in plateau, *Fuel*, 381:133492.

[8] Kan, Z.C., Hu, Z.Y., Lou, D.M., Tan, P.Q., Cao, Z.Y. and Yang, Z.H. 2018. Effects of altitude on combustion and ignition characteristics of speed-up period during cold start in a diesel engine, *Energy*, 150:164–175.

[9] Zhao, L.Y., Lei, J.L., Liu, Y., Deng, W. and Yang, L.J. 2024. Energy-based cold-start strategies for diesel engines at extreme low temperature, *Thermal Science and Engineering Progress*, 47: 102274.

[10] He, X., Zhou, Y., Liu, Z.C., Yang, Q., Sjöberg, M., Vuilleumier, D., Ding, C.P. and Liu FS. 2022. Impact of coolant temperature on the combustion characteristics and emissions of a stratified-charge direct-injection spark-ignition engine fueled with E30, *Fuel*, 309:121913.

[11] Knothe, G. and Razon, L.F. 2017. Biodiesel fuels, *Progress in Energy and Combustion Science*, 58(1):36-59.

[12] Davanlou, A., Lee, J.D., Basu, S. and Kumar, R. 2015. Effect of viscosity and surface tension on breakup and coalescence of bicomponent sprays, *Chemical Engineering Science*, 131:243-255.

[13] Zigan, L., Shi, J.M., Krotow, I., Schmitz, I., Wensing, M. and Leipertz, A. 2013. Fuel property and fuel temperature effects on internal nozzle flow, atomization and cyclic spray fluctuations of a direct injection spark ignition-injector, *International Journal of Engine Research*, 14(6):543-556.

[14] Pan, M., Huang, R., Liao, J., Jia, C., Zhou, X., Huang, H. and Huang, X. 2019. Experimental study of the spray, combustion, and emission performance of a diesel engine with high n-pentanol blending ratios, *Energy Conversion and Management*, 194:1-10.

[15] Yassine, E.I.M. and Joonsik, H. 2024. Microscopic Imaging on Diesel Spray and Atomization Process, *Processes*, 12(2):2227-9717.

[16] Hawi, M., Kosaka, H., Sato, S., Nagasawa, T., Elwardany, A. and Ahmed, M. 2019. Effect of injection pressure and ambient density on spray characteristics of diesel and biodiesel surrogate fuels, *Fuel*, 254:115674.

[17] Algayyim, S.J.M. and Wandel, A.P. 2021. Macroscopic and microscopic characteristics of biofuel spray (biodiesel and alcohols) in CI engines: A review, *Fuel*, 292:120303.

[18] Li, Y.T., Huang, Y.C., Yang, S.S., Luo, K., Chen, R.X. and Tang, C.L. 2019. A comprehensive experimental investigation on the PFI spray impingement: Effect of impingement geometry, cross-flow and wall temperature. *Applied Thermal Engineering*, 159:113848.

[19] Gilles, B., Mickael, C. and Alaa, O. 2012. Air Entrainment in Diesel-Like Gas Jet by Simultaneous Flow Velocity and Fuel Concentration Measurements, Comparison of Free and Wall Impinging Jet Configurations, *SAE International Journal of Engines*, 5(2):76-93.

[20] Ali, M., Yoshiyuki, K. and Kei, M. 2002, Effect of Injection Parameters and Wall-Impingement on Atomization and Gas Entrainment Processes in Diesel Sprays, *SAE Transactions*, 111:1070-1079.

[21] Djamari, D.W., Idris, M., Paristiawan, P.A., Abbas, M.M., Samuel, O.D., Soudagar, M.E.M., Herawan, S.G., Chandran, D., Yusuf, A.A., Panchal, H. and Veza, I. 2022. Diesel Spray: Development of Spray in Diesel Engine, *Sustainability*, 14(23): 15902.

[22] He, X., Xu, K., Liu, Y.L., Zhang, Z., Zhang, H. and Zhao, J. 2023. Effects of ambient density and injection pressure on ignition and combustion

characteristics in diesel spray under plateau cold-start conditions, *Fuel*, 352:129039.

[23] Du, W., Zhang, Q.K., Zhang, Z., Lou, J.J. and Bao, W.H. 2018. Effects of injection pressure on ignition and combustion characteristics of impinging diesel spray, *Applied Energy*, 226:1163-1168.

[24] Shi, Z.C., Wu, H., Li, H.Y., Zhang, L., Li, X.G. and Lee, C.F. 2021. Effect of injection pressure and fuel mass on wall-impinging ignition and combustion characteristics of heavy-duty diesel engine at low temperatures, *Fuel*, 299:120904.

[25] Liu, F.S., Yang, Z.M., Li, Y.K. and Wu, H. 2019. Experimental study on the combustion characteristics of impinging diesel spray at low temperature environment, *Applied Thermal Engineering*, 148:1233-1245.

[26] Ma, F.K., Xu, R.F. and Liu, X.Y. 2024. Fuel injection performance and spray characteristic of high-pressure common rail systems at low temperatures, *Energy Science & Engineering*, 12(3):1233-1241.

[27] Wang, Z.M., Jiang, C.Z., Xu, H.M. and Wyszynski, M.L. 2016. Macroscopic and microscopic characterization of diesel spray under room temperature and low temperature with split injection, *Fuel Processing Technology*, 142:71-85.

[28] Wei, Y., Li, T., Zhou, X. and Zhang, Z. 2020. Time-resolved measurement of the near-nozzle air entrainment of high-pressure diesel spray by high-speed micro-PTV technique, *Fuel*, 268:117343.

[29] Park, S.H., Kim, H.J., Suh, H.K. and Lee, C.S. 2009. Experimental and numerical analysis of spray-atomization characteristics of biodiesel fuel in various fuel and ambient temperatures conditions, *International Journal of Heat and Fluid Flow*, 30(5): 960-970.

[30] Kyungwon, L., Dario, L.P., Dimitris, A., Seokwon, C. and Joonsik, H. 2023. Fuel temperature and injection pressure influence on the cold start GDI sprays, *Applications in Energy and Combustion Science*, 16:100206.

[31] Li, J.Y., Wang, X.Y., Yu, H.Z.N., Liu, Y., An, X.P., Ma, K.Q., Liang, Y.K., Xu, H. and Zhang, H. 2023. The Investigation of the Mixture Formation and Combustion Characteristic of the Spray-wall Impingement, *Journal of Physics: Conference Series*, 2491:012025.

[32] Liu, R., Huang, L., Yi, R., Xia, J., Zhang, J., Feng, M.Z. and Lu, X.C. 2024. Visualization on spray and flame characteristics of wall-impinging spray under marine diesel engine conditions, *Applied Thermal Engineering*, 244:122655.

[33] Yang, C., Cheng, X.B., Li, Q.Q. and Wang, Y.D. 2023. Experimental study on the interactions of wall temperature and impingement distances and their effects on the impinged diesel spray ignition and combustion characteristics, *Applied Thermal Engineering*, 230:120670.

[34] Dai, M., Akira, A., Akari, S., Eriko, M. and Jiro, S. 2024. Experimental analysis of spray impingement wall film at cold temperatures for Direct-Injection spark ignition engines, *Fuel*, 374:132407.

[35] Wang, X.R., Li, H.G., Li, G.X., Fan, J.T., Bai, H.L., Gao, Y. and Huo, H.B. 2024. Effect of injection pressure on low-temperature fuel atomization characteristics of diesel engines under cold start conditions, *International Journal of Multiphase Flow*, 172:104712.

[36] Bothell, J.K., Machicoane, N., Li, D., Morgan, T.B., Aliseda, A., Kastengren, A.L. and Heindel, T.J. 2020. Comparison of X-ray and optical measurements in the near-field of an optically dense coaxial air-assisted atomizer, *International Journal of Multiphase Flow*, 125:103219.

[37] Chen, R., Nishida, K. and Shi, B. 2019. Quantitative investigation on the spray mixture formation for ethanol-gasoline blends via UV-Vis dual-wavelength laser absorption scattering (LAS) technique, *Fuel*, 242:425–437.

[38] Chen, H.Y., Shi, Z.J., Liu, F.S., Wu, Y. and Li, Y.K. 2022. Non-monotonic change of ignition delay with injection pressure under low ambient temperature for the diesel spray combustion, *Energy*, 243: 123017.

[39] Lei, J.L., Li, J.W. and Liu, Yi. 2022. Ethanol drop impingement on ultracold surfaces under low-temperature cold-start conditions of engines, *Fuel*, 311:122573.

[40] Xin, S.R., Wang, W.Y., He, Y., Zhu, Y.Q. and Wang ZH. 2024. Effect of low fuel temperature on combustion deterioration of kerosene swirling spray flames using OH-PLIF, *Fuel*, 358: 130098.

7 CONTACT

Lilyzhao004@163.com(Liyan. zhao);

leijilin@kmust.edu.cn(Jilin. Lei);

lqyi@kust.edu.cn (Yi. Liu).